Assessment of periapical lesions by 7T magnetic resonance imaging and micro-CT - experimental study

[1]Antonela M. Berar, [2]Dan Preda, [1]Simona Iacob, [3]Corina V. Moraru, [3]Alexandru Farcasanu, [3]Flaviu R. V. Turcu, [3,4]Simion Simon, [1]Smaranda Buduru

[1]Department of Prosthodontics, Faculty of Dental Medicine, "Iuliu Hatieganu" University of Medicine and Pharmacy, Cluj-Napoca, Romania; [2]Radiology and Medical Imaging Laboratory, County Clinical Emergency Hospital, Cluj-Napoca, Romania; [3]National Centre of Magnetic Resonance, Faculty of Physics, Babes-Bolyai University, Cluj-Napoca, Romania; [4] Nanostructured Materials and Bio-Nano-Interfaces Center, Interdisciplinary Research Institute on Bio-Nano-Sciences, Babes-Bolyai University, Cluj-Napoca, Romania.

Abstract. Introduction: The currently existing imaging methods provide the opportunity to investigate even deeply the periapical lesions (PL). The objective of the study was to highlight the qualitative changes detected on 7 T MRI and micro-CT in model rats with experimentally induced PL. Material and methods: Four groups of animals were used: control group (C), experimentally induced PL group (PL), diabetes mellitus and PL group (PLD) and postmenopausal osteoporosis treated with zoledronic acid and PL group (PLO). All the animals were investigated at 14, 30 and 60 days by using MRI at a magnetic field strength of 7 Tesla and by micro-CT scanning and histopathological examination only for the group with PL, at 30 days. Results: The PL was identified based on the MRI and micro-CT images. The periapical inflammation was visible early in the axial and coronal MRI sections and appeared in marked hypersignal in the PLD group compared with the other groups of animals. Conclusion: MRI is a non-radiating method that allows *in vivo* early detection of PL and offers the possibility to study its evolutions in a continuous manner. Micro CT has the advantage of a high-resolution, providing detailed images of teeth and periapical structures, but it is expensive, time consuming and can only be used *in vitro*. Mostly micro-CT that are used in laboratories are for in vitro studies. If the two imaging modality would allow in vivo PL investigation, both can offfer complementary views on the PL evolution.

Key Words: magnetic resonance imaging, micro-CT, periapical lesion.

Corresponding Author: S. Buduru; e-mail: dana.buduru@umfcluj.ro

Introduction

Periapical lesions (PL) are induced by endodontic bacteria and produce changes in the apical area of the teeth, involving periapical tissue inflammation and alveolar bone damage (Nair 2006). Different radiographic and imaging methods such as digital radiography, computed tomography (CT) with multiple detectors, or cone-beam computed tomographic (CBCT) are used to assess alveolar bone loss caused by PL (Vandenberghe et al 2010, Gaudino et al 2011). Magnetic resonance imaging (MRI) is an imaging technique used in dentistry to investigate the temporomandibular joint structures, rarely employed in endodontics (Geibel et al 2014, Senthilkumaran et al 2014, Klein HM 2016). However, due to its high sensitivity in detecting inflammation, MRI can be an adjuvant imaging method to visualize the characteristics of pathological processes located in the jaw bones and teeth, such as inflammatory pulpal pathology, vascularization of dental pulp after trauma and inflammatory periapical diseases. Thus, dental structures such as dental roots, pulp chamber and dentin can be very well visualized by MRI. The periodontal ligament, cortical / cancellous bone, and lamina dura, difficult to see on CT images, can be better visualized by MRI (Gaudino et al 2011).
Microcomputed tomography (micro-CT) is a novel imaging technology, frequently used to evaluate bone morphology in small animals. It is a method that accurately detects alveolar bone loss (Oliveira et al 2015). In addition, it is an imaging technique that provides high-resolution 2D and 3D images for good multiplanar evaluation of PL (Kalatzis-Sousa et al 2016). Micro-CT has been used to assess periapical bone destruction, providing results equivalent to those obtained in the histological evaluation of these lesions (Balto et al 2000).
Currently, micro-CT is used in research studies for the *in vitro* quantification of changes in bone architecture and on small specimens because of the high dose of radiation, which is not compatible with living organisms. However, there is interest on developing a low radiating micro CT to be used *in vivo* (von Stechow et al 2003).
Diabetes mellitus (DM) has an influence on the evolution of PL. A systematic review and meta-analysis on most relevant research suggested a connection between the existence of periapical radiolucency in root filled teeth among diabetics (Gupta

et al 2020). To our knowledge there are not many studies assessing the DM influence on PL using MRI.
Osteoporosis can cause altered dental health. A recent study shows that PL are more statistically significant in patients with osteoporosis (Katz et al 2021). Both PL and osteoporosis are characterized by bone resorption and studies on rats have showed that the evolution of apical periodontitis depends on the resorptive process of the alveolar process. In addition, the decrease of the estrogen level causes an increase of the resorptive activity in bones (Holland et al 2017, Xiong et al 2007). The role of the proinflammatory cytokines such as IL-6 was studied in bone resorption in induced osteoporosis on ovariectomized female rats treated with bisphosphonates. An increased level of circulating IL-6 was correlated with decreased bone density (Berar et al 2020).
The objective of the study was to highlight the qualitative changes detected on 7T MRI and micro-CT in model rats with experimentally induced PL.

Materials and Methods

The procedures on animals were carried out with the approval of the Ethical Commission of Iuliu Hatieganu University of Medicine and Pharmacy, Cluj-Napoca and respecting the international norms regarding the research on animals for scientific purposes.

Experimentally induced PL examined by MRI

The imaging examinations by magnetic resonance were performed at the National Center for Magnetic Resonance from the Faculty of Physics, University Babes-Bolyai, Cluj-Napoca. Thirty-two animals were distributed in four groups: control group (C) - 2 animals, PL group - 10 healthy male rats with experimentally induced lesions in the right mandibular M1 teeth, PLD group - 10 male rats with experimental diabetes mellitus and PL and PLO group - 10 female rats with postmenopausal osteoporosis treated with zoledronic acid and PL.
The MRI experiment was done on a Bruker Biospec 7.04 Tesla (Ettlingen, Germany) a horizontal small animal MRI scanner system equipped with a BGA-9S gradient system (760 mT/m maximum gradient strength). A RF RES 300 MHz 1H 089/040 quadrupolar coil with an active diameter of 40 mm was used for the transmission and reception of the radio frequency signal. The animals were investigated at 14, 30 and 60 days.
Before the scan, the animals were anesthetized with a mixture of ketamine (Vetased, SC Pasteur-Filipeşti SRL) 0.1 ml / kg body and xylazine hydrochloride (Alfasan International BV, The Netherlands) 0.05 ml / kg body weight, intramuscularly administered.
During the scan, the animals were tracked using a small animal monitoring device (1225T Monitoring & Gating System, Small Animal Instruments, Inc, NY). The electrocardiogram, temperature and respiratory rate were monitored.
The contrast agent - MAGNEVIST® (Bayer Schering Pharma AG) was administered into the femoral vein at a concentration of 0.2 ml / kg body weight. Animals were positioned in the quadrupole volume coil (RF RES 300 MHz 1H 089/040 QUAD TR. Post-injection of gadolinium-based contrast agent the images were obtained using the RARE acquisition sequence (Rapid Acquisition with Relaxation Enhancement) - weighted - T1 (longitudinal relaxation time of hydrogen protons), which was performed after selecting the following parameters: repetition time (TR) 1300 ms, echo time (TE) 9.5 ms, visual field (FOV) 1x1cm, matrix 256x256, section thickness of 0.5 mm. The images were acquired in the sagittal, coronal and axial planes, and the scanning time was of 10 minutes.
The MRI images were then analyzed by a radiologist with competence in magnetic resonance and a dento-alveolar surgeon, using the image visualization software RadiAnt Dicom Viewer v.1.9.

Experimentally induced PL examined by micro-CT imaging

Micro-CT scanning was performed in the Experimental Medicine Center of Iuliu Hațieganu University of Medicine and Pharmacy, Cluj-Napoca.
The study included the animals from the PL group, with lesions induced in the right mandibular M1 teeth, after the experimental exposure of the dental pulp to the salivary environment for 30 days. The left mandibular M1 teeth was used as the control. At the end of the experimental period and after euthanizing the animals, the mandibular pieces were introduced in 10% formaldehyde solution, and after an interval of 24 hours the soft tissues were washed and removed.
Hemimandibules were imagistically examined by micro-CT. The microtomographic investigation of the M1 and PL was performed using the micro-CT Scanner SkyScan 1072 ® (80 kV, 125 mA). The pieces were scanned after adjusting the acquisition parameters of the device. Thus, approximately 200 microtomographic sections were obtained in a .bmp format for each piece. The total scanning time for each specimen was of approximately 2 hours. The images were visualized with the Data Viewer software v.1.5, and after scanning, the three-dimensional reconstructions of the right hemi-mandibules were obtained in the animals with PL and in the control ones with the CT software vox v.2.7.

Experimentally induced PL examined by histopathological analysis

The animals were sacrificed, and their mandibular jaws were chemically fixed by immersion in 4% buffered formaldehyde for 48 hours. Decalcification of the samples was performed by treating the fixed parts with formic acid/hydrochloric acid (1/1), diluted 8% for 4 weeks. After decalcification, the samples were subjected to the classical paraffin embedding technical process. This technique consists in carrying out standard steps: washing, dehydration in successive 70%, 80%, 90% and absolute alcohol baths, followed by the inclusion in 62^{O}C paraffin under vacuum for 6 hours, using a paraffin with a high melting point. After inclusion, the samples were sectioned at a 4 µm thickness. The next steps consisted in deparaffining the samples in 100% xylene, hydrating in 100%, 96% and 70% alcohol baths, followed by staining with hematoxylin eosin.

Results

Analysis of the results obtained by MRI examination

Magnetic resonance imaging was acquired in the RARE T1 sequence in 3 spatial planes, based on the previously mentioned parameters, post-administration of contrast agent. Axial and coronal planes are the planes of choice, which best highlight pathological lesions and anatomical regions. The images obtained in

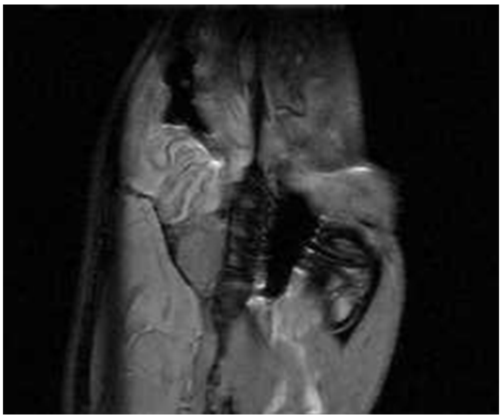

Fig. 1. Sagital section MRI of the right mandibular molar

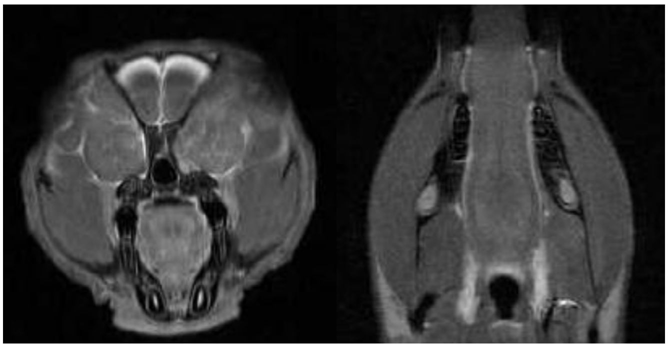

Fig. 2. Axial and coronal MRI sections, group C

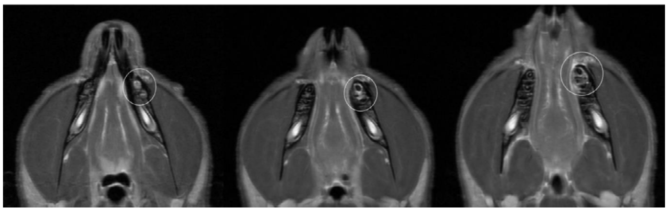

Fig.3. Successive coronal mandibular molar MRI sequences, time 30 days

Fig. 4. Successive coronal mandibular molar MRI sequences, time 14 days

Fig. 5. Successive coronal mandibular molar MRI sequences, time 30 days.

the sagittal plane were not relevant in highlighting PL in the first mandibular molars, as they did not allow a comparative analysis of the intrinsic appearance of the altered tissues on the right side, compared to the normal ones on the left side (Figure 1). Axial and coronal images, post-injection of contrast agent, provide information about the PL extension and allow direct comparison between the right side with the lesion, compared to the contralateral side, normal.

Group C

The symmetry of the signal obtained at the level of apical and periapical tissues from the bilateral molar region, on axial and coronal images is observed in Figure 2.

Group PL

At 14 days: The lesions were visible as an inhomogeneous, invasive structure of the surrounding anatomical tissues, with an infiltrative character, and imprecise delimitation. Qualitative structural changes were detected around the periradicular region of mandibular M1 molar, suggestive for the presence of a local inflammatory process. The local inflammation caused an increase in the concentration of the contrast substance at this level, which determined the appearance of the hypersignal visible on images in the RARE T1 sequence. Postcontrast the paramagnetic substance is moderately and nonhomogeneously captured by the mentioned lesions.

At 30 days: The diffuse extension of the lesions begins to narrow, the delimitation is more precise, the location is mainly in the periapical region, the detected signal being more intense compared with the left side, and the affected area in hypersignal. Postcontrast, in the affected area the detected signal is slightly increased (Figure 3).

At 60 days: The granulation tissue is visualized on the axial and coronal images, and the vestibular and lingual cortices in the M1 region are not affected. Postcontrast, there is a decrease of the signal in the granulation tissue.

Group PLD

At 14 days: In the periapical region there is an inhomogeneous structure with diffuse delimitation, moderate mass effect on adjacent anatomical structures, with peripheral extension to the subcutaneous level. There is a diffuse edema, more pronounced perilesional, that extends around, being more visible in the surrounding soft parts. The lesion, together with the edema, gives the anatomical region a ballooned appearance, compared to the left, contralateral, normal side. Periosteal destruction with insular appearance is observed in the pathological area (Figure 4).

At 30 days: Compared to the 14-day imaging examination, the hypersignal is diminished with a medium intensity, which corresponds to a reduced edema. There is also a reduction of the mass effect (Figure 5).

At 60 days: Periradicular hypersignal is detected on the RARE T1 sequence, with minimal edema and minimal mass effect on adjacent soft tissues.

Group PLO

At 14 days: On RARE T1 sequences (native and postcontrast) the imaging changes are visible, with minimal signal changes in the axial and coronal planes.

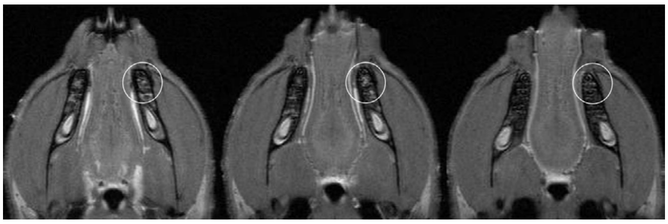

Fig. 6. Successive axial mandibular molar MRI sequences, time 30 days.

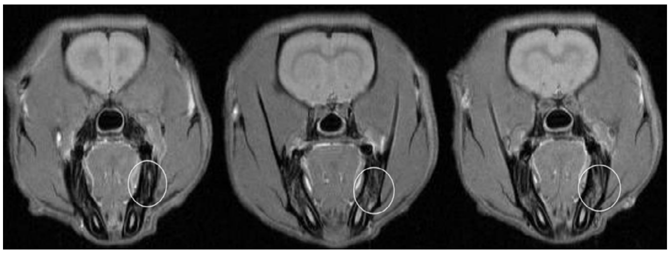

Fig. 7. Successive coronal mandibular molar MRI sequences, time 60 days

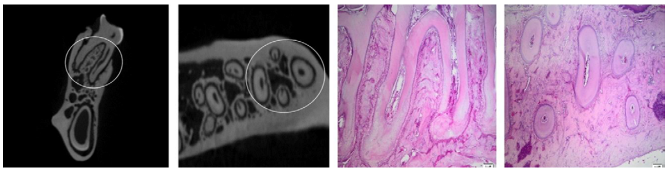

Fig. 8. Micro-CT images and histopathological sections (HE stain) of the periapical region at the left mandibular M1, healthy animals

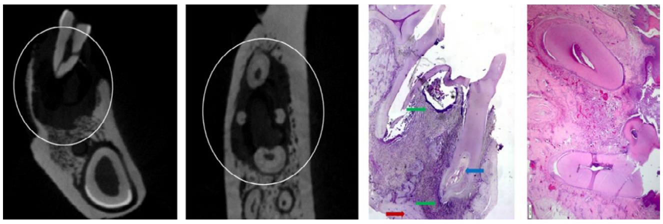

Fig. 9. Right mandibular M1 micro-CT images in animals with PL/ Histopathological images: pulpal necrosis (blue arrow), chronic extended periodontitis (green arrow) and mandibular bone resorption (red arrow)

At 30 days: The images made in the axial and coronal planes show the same minimal changes, on the sequences mentioned above (Figure 6).
At 60 days: Imaging changes are much reduced compared to those at 14 and 30 days on the aforementioned sequences in the axial and coronal planes (Figure 7).

Analysis of the results obtained by micro-CT examination
By micro-CT analysis performed on all specimens collected at 30 days, high-resolution images were obtained, which show in most detail the normal and pathological periapical structures at the level of the mandibular molars. The left mandibular pieces obtained from healthy animals show an uniform periodontal space, of normal width, integral lamina dura, and periradicular alveolar bone of normal appearance both on micro-CT and histopathological images (Figure 8).
The experimental right mandibular samples with first molar pulp exposed to the salivary environment, presented a significant periapical radiotransparency around affected roots. The mesio-distal extension observed on the micro-CT sections of the periapical lesion was larger than the vestibulo-lingual extension (Figure 9). The histopathological investigations showed necrotic pulp chambers with microbial colonization, dentinal microbial invasion with dentinal lagunes and caverns, extensive apical and periodontal abscesses, periodontal granulomas with osteoclasts and conjunctive granulation tissue. Microscopic images showed PL characterized by extensive bone resorption by osteoclasts and connective tissue. Chronic periodontitis of the peri and interradicular ligaments at the level of soft tissues was also present, as it can be observed in Figure 9.

Discussions

The imaging examinations have an important role in establishing the diagnosis of PL of endodontic origin. The two imaging methods used in this study for the assessment of PL induced on rat models produce the images without the overlap of the tissues and are based on different techniques: on one hand, MRI operating with the magnetic field, without using ionizing radiation and on the other hand micro-CT imaging using X-rays, both methods aiming and contributing to the improvement of the PL diagnosis (Mendes et al 2020).
MRI is an useful investigation method that provides a detailed analysis of soft dental and soft adjacent tissues and a staging based on the degree of tissues damage. Dental mineralized tissues cannot be accurately detected by MRI because of the low content of water within the enamel and dentin microstructure, and the water molecules in the dentinal canals have a short T2 relaxation time, causing a decreased MRI signal when using standard techniques like spin echo or gradient echo. This can be improved by using special acquisition techniques or by increasing the signal from these tissues or using a stronger magnetic field (Di Nardo et al 2018, Sustercic et al 2012, Weglarz et al 2003). Normal and pathological dental tissues appear in MRI images as shades of gray on a white to black scale, corresponding to hypersignal (white), hyposignal (black) or intermediate signal (gray), depending on the acquisition sequence of images. Dental structures such as enamel and dentin appear in hyposignal due to the lack of hydrogen protons. The dental pulp appears in hypersignal or intermediate signal, using the T1 sequence. The cortical bone is visualized in hyposignal delimited by an intermediate signal given by the adjacent soft tissues. In PL associated with alveolar bone destruction, T1 images show an area in hyper or moderate signal, different from the surrounding normal bone, the signal variation being related to the presence of the inflammatory exudate in the lesions (Tutton et al 2002). A higher sensitivity was observed when using MRI compared to CBCT in diagnosing periapical lesions. Some authors suggested that inflammatory pathologies in dental tissues can be identified in an earlier phase with MRI compared to CBCT or classical radiography. MRI proved to be useful to investigate the decay extensions (Bracher et al 2013), the vitality of the dental pulp, microcracks, fractures or root canals (Di Nardo et al 2018).
MRI images have the advantage of early detection and visualization of the lesions in all groups of animals. In MRI, several acquisition plans and sequences of radio magnetic pulses can be used, which help to stage the evolution of PL. Although the

costs of MRI examination are higher than those of radiological examinations, the advantages of interpreting the images are clearly superior, facilitating staging and orientation towards an appropriate therapy (Patil 2021). MRI is not a radiating method and allows the in vivo detection of PL. This is a feature that permits acquisition of multiple images at different moments to evaluate the progression of inflammation.

In this study, the signal intensity in the region of interest compared to the adjacent tissues was different in three groups of animals (PL, PLD and PLO). MRI images showed hypersignal suggesting the presence of the inflammatory process in the lesions, more intense in the PLD group. The most relevant MRI examination of the lesions was at 14 days after the experimental induction. This is due to the edema present at the initial moment, which is easily highlighted on MRI, and it is specific to the active stage of the lesions, as opposed to the chronic stage, where the content of water molecules is much lower. The most expressed imaging changes were noticed in the case of animals with DM and PL. These results are in accordance with other studies, which confirm the effect of DM on the development of PL, experimental studies reporting similar results of intense periapical inflammatory infiltrate with more bone resorption in diabetic animals compared with controls (Liz Pérez-Losada et al 2020, Patil et al 2021, Berar et al 2016, Cintra et al 2014). It is known that diabetes lowers tissue repair capability mostly as a consequence of the accumulation of glycation end products that can cause inflammation continued with bone resorption. Pro-inflammatory cytokines are increased, determining repair capacity and immune reaction to be hazardous, respecting the periapical condition (Asadipooya et al 2019). Oxidative stress parameters are also modified during the inflammatory process of the PL (Berar et al 2015). A study on the prevalence of apical periodontitis in patients with DM having optimal or poor glycemic control compared with nondiabetics was done using CBCT and showed that the prevalence of PL and severe bone destruction in periapical tissues was significantly lower in the nondiabetic patients compared with DM patients. No difference was observed between poor or optimal control of diabetes. To mention that it is also highlighted that PL can be a source of infection of other sites in the organism and can aggravate the symptoms of DM (Sisli at al 2019).

Among the imaging methods used in this study, the micro-CT was efficient in rendering the fine details of the periapical anatomical and pathological structures, the images accurately showed the contour and size of PL. In addition, micro-CT imaging allows an objective determination of the real extent of the lesions. Mineralized tooth tissues and alveolar bone are accurately detected on high-resolution micro-CT images. However, the drawback lies in its invasiveness, time consuming and not being an in vivo analysis plus that it uses harmful ionizing radiation. In other relevant studies, micro-CT images may be useful for the assessment of PL, especially periradicular alveolar destruction (Kalatzis-Sousa et al 2016, de Oliveira et al 2015, Stechow et al 2003). Histological methods are considered golden standard in emphasizing changes at tissue level and shows the invasiveness of inflammation. The radiotransparency observed in micro-CT images correspond to the alveolar bone resorption caused by osteoclasts which is replaced with by the granulation tissue overlapped with the different degree of inflammation according to the stage of lesion. To mention that external roots resorption, including destruction of radicular dentin and cementum could be very well identified on the histopathological sections (Berar et al 2016).

Conclusions

Both imaging methods have proved the utility in detection and visualization of the qualitative changes of periapical structures, offering complementary aspects for diagnostic purpose in PL. Magnetic resonance imaging provides an *in vivo*, non-invasive, radiation free investigation to identify the lesions from the earliest stages and to distinguish different phases in the development of PL. Micro-CT allows an *in vitro* detailed qualitative assessment of the teeth and PL, demonstrating a high diagnostic accuracy. Considering the obtained results, we conclude that MRI has clinical significance, establishing the damage degree of the supporting tissue of the teeth as early as possible, individualizing the diagnosis and directing to an accurate treatment.

References

Asadipooya K, Uy EM. Advanced Glycation End Products (AGEs), Receptor for AGEs, Diabetes, and Bone: Review of the Literature. J Endocr Soc 2019;10;3(10):1799-1818.

Balto K, Müller R, Carrington DC, Dobeck J, Stashenko P. Quantification of periapical bone destruction in mice by micro-computed tomography. J Dent Res 2000;79:35-40.

Berar AM, David DC, Lascu L, Matros L, Campian RS. Analysis of hematological and oxidative stress parameters in the evaluation of experimentally induced periapical lesions. HVM Bioflux 2015;7(3):162-167.

Berar AM, Kui AI, Moraru CV, Matros L, Picos A, Lascu L, Campian RS. A quantitative radiological and histopathological study of periapical inflammatory lesions associated with experimentally induced diabetes and osteoporosis. HVM Bioflux 2016;8(2):85-91.

Berar AM, Buduru S, Mârza TV, Iacob S, David DC, Matros L, Constantiniuc M. Increased serum of interleukin 6 in experimental periapical periodontitis associated with metabolic bone disease. Health, Sports & Rehabilitation Medicine 2020;21(1):28-32.

Cintra LT, Samuel RO, Facundo AC, Prieto AK, Sumida DH, Bomfim SR, et al. Relationships between oral infections and blood glucose concentrations or HbA1c levels in normal and diabetic rats. Int Endod J 2014;47,228–237.

Perez-Losada FDL, Estrugo-Devesa A, Castellanos-Cosano L, Segura-Egea JJ, López-López J, Velasco-Ortega E. Apical Periodontitis and Diabetes Mellitus Type 2: A Systematic Review and Meta-Analysis. J Clin Med 2020;9,540.

Gaudino C, Cosgarea R, Heiland S, Csernus R, Beomonte ZB, Pham M, et al. MR-Imaging of teeth and periodontal apparatus: an experimental study comparing high-resolution MRI with MDCT and CBCT. Eur Radiol 2011;21:2575-83.

Gupta A, Aggarwal V, Mehta N, Abraham D, Singh A. Diabetes mellitus and the healing of periapical lesions in root filled teeth: a systematic review and meta-analysis. Int Endod J 2020; 53(11):1472-1484.

Holland R, Gomes FJE, Cintra LTA. Queiroz IOA, Estrela C. Factors affecting the periapical healing process of endodontically treated teeth. J Appl Oral Sci 2017;25(5):465-76.

Kalatzis-Sousa NG, Spin-Neto R, Wenzel A, Tanomaru-Filho M, Faria G. Use of micro-computed tomography for the assessment of periapical lesions in small rodents: a systematic review. Int Endod J 2017;50,4:352-366.

Oliveira, KMHD, Nelson-Filho P, da Silva LAB, Küchler EC, Gatón-Hernandez P & da Silva RAB. Three-Dimensional Micro-Computed Tomography Analyses of Induced Periapical Lesions in Transgenic Mice. Ultrastruct Pathol 2015;39:6,402-407.

Katz J, Rotstein I. Prevalence of Periapical Lesions in Patients with Osteoporosis. J Endod 2021;47(2):234-238.

Klein, Hans-Martin. Clinical low field strength magnetic resonance imaging: a practical guide to accessible MRI. Springer, 2015.

Nair PNR. On the causes of persistent apical periodontitis: A review. Int Endod J 2006;39:249-281.

Oliveira KMH, Nelson-Filho P, da Silva LAB, Küchler EC, Gat n-Hernandez P, da Silva RAB. Three-Dimensional Micro-Computed Tomography Analyses of Induced Periapical Lesions in Transgenic Mice. Ultrastruct Pathol 2015;39(6):402-407.

Patil S, Alkahtani A, Bhandi S, Mashyakhy M, Alvarez M, Alroomy R, Hendi A, Varadarajan S, Reda R, Raj AT et al. Ultrasound Imaging versus Radiographs in Differentiating Periapical Lesions: A Systematic Review. Diagnostics 2021;11:1208.

Silwan Mendes, Carin A. Rinne, Julia C. Schmidt, Dorothea Dagassan-Berndt, Clemens Walter. Evaluation of magnetic resonance imaging for diagnostic purposes in operative dentistry - a systematic review. Clin Oral Investig 2020;24:547–557.

Sisli SN. Evaluation of the Relationship between Type II Diabetes Mellitus and the Prevalence of Apical Periodontitis in Root-Filled Teeth Using Cone Beam Computed Tomography: An observational cross-sectional study. Med Princ Pract 2019;28:533–538.

Sustercic D, Sersa I. Human tooth pulp anatomy visualization by 3D magnetic resonance microscopy. Radiol Oncol 2012;46(1):1-7.

Tutton LM, Goddard PR. MRI of the teeth. Br J Radiol 2002;75(894):552-562.

Vandenberghe B, Jacobs R, Bosmans H. Modern dental imaging: A review of the current technology and clinical applications in dental practice. Eur Radiol 2010;20(11):2637–55.

Von Stechow D, Balto K, Stashenko P, Müller R. Three-dimensional quantitation of periradicular bone destruction by micro-computed tomography. J Endod 2003;29(4):252-256.

Xiong H, Peng B, Wei L, Zhang X, Wang L. Effect of an estrogen-experimental periapical lesions in rats. J Endod 2007;33(11):1304.

Authors

•Antonela Marcela Berar, Department of Prosthodontics, Faculty of Dental Medicine, Iuliu Hatieganu University of Medicine and Pharmacy, 32 Clinicilor Street, Cluj-Napoca, Romania, e-mail: antonela_berar@yahoo.com

•Dan Preda, Radiology and Medical Imaging Laboratory, County Clinical Emergency Hospital, 3-5 Clinicilor Street, Cluj-Napoca, Romania, e-mail: dp56dr@yahoo.com

•Simona Iacob, Department of Prosthodontics, Faculty of Dental Medicine, Iuliu Hatieganu University of Medicine and Pharmacy, 32 Clinicilor Street, Cluj-Napoca, Romania, e-mail: simona72cj@yahoo.com

•Corina Violeta Moraru, National Centre of Magnetic Resonance, Faculty of Physics, Babes-Bolyai University, 1 Mihail Kogălniceanu Street, Cluj-Napoca, Romania, e-mail: corina_hebristean@yahoo.co.uk.

•Alexandru Farcasanu, National Centre of Magnetic Resonance, Faculty of Physics, Babes-Bolyai University, 1 Mihail Kogălniceanu Street, Cluj-Napoca, Romania, e-mail: stefan.farcasanu@gmail.com

•Flaviu Romulus Valeriu Turcu, National Centre of Magnetic Resonance, Faculty of Physics, Babes-Bolyai University, 1 Mihail Kogălniceanu Street, Cluj-Napoca, Romania, e-mail: fturcu@phys.ubbcluj.ro.

•Simion Simon, National Centre of Magnetic Resonance, Faculty of Physics, Babes-Bolyai University and Nanostructured Materials and Bio-Nano-Interfaces Center, Interdisciplinary Research Institute on Bio-Nano-Sciences, Babes-Bolyai University, 1 Mihail Kogălniceanu Street, Cluj-Napoca, Romania Cluj-Napoca, Romania, email: simon49nmr@gmail.com

•Smaranda Buduru, Department of Prosthodontics, Faculty of Dental Medicine, Iuliu Hatieganu University of Medicine and Pharmacy, 32 Clinicilor Street, Cluj-Napoca, Romania, e-mail: dana.buduru@umfcluj.ro

Citation	Berar AM, Preda D, Iacob S, Moraru CV, Farcasanu A, Turcu DRV, Simon S, Buduru S. Assessment of periapical lesions by 7T magnetic resonance imaging and micro-CT - experimental study. HVM Bioflux 2022;14(1):10-15.
Editor	Antonia Macarie
Received	5 December 2021
Accepted	16 January 2022
Published Online	29 January 2022
Funding	None reported
Conflicts/ Competing Interests	None reported